International Journal of Mechanical, Industrial and Aerospace Sciences
ISSN: 2517-9950
Vol:6, No:4, 2012

Proposal of a Means for Reducing the Torque Variation on a Vertical-Axis Water Turbine by Increasing the Blade Number

M. Raciti Castelli, S. De Betta and E. Benini

***Abstract*—**This paper presents a means for reducing the torque variation during the revolution of a vertical-axis water turbine (VAWaterT) by increasing the blade number. For this purpose, two-dimensional CFD analyses have been performed on a straight-bladed Darrieus-type rotor. After describing the computational model and the relative validation procedure, a complete campaign of simulations, based on full RANS unsteady calculations, is proposed for a three, four and five-bladed rotor architectures, characterized by a NACA 0025 airfoil. For each proposed rotor configuration, flow field characteristics are investigated at several values of tip speed ratio, allowing a quantification of the influence of blade number on flow geometric features and dynamic quantities, such as rotor torque and power. Finally, torque and power curves are compared for the three analyzed architectures, achieving a quantification of the effect of blade number on overall rotor performance.

***Keywords*—**Vertical-Axis Water Turbine, rotor solidity, CFD, NACA 0025

I. Introduction and Background

THE original concept of the Darrieus turbine was patented in the USA in 1931. Its aim was to produce wind energy for electrical power generation [1]. Darrieus patent employed a set of curved blades approximating the shape of a perfectly flexible cable, namely the Troposkien shape [2]. Later, vertical axis designs, comprising straight bladed architectures, appeared under different names, such as “H-Darrieus” or “Squirrek Cage Darrieus” turbines [3]. Modifications of the Darrieus turbine to extract energy from rivers and tidal streams rather than wind has attracted a number of international researchers, leading to a growing interest in Darrieus-type tidal or current turbines, which may operate in river, tidal or marine current flows by directly converting the kinetic energy of the free stream into electricity with no need for a static pressure head across the turbine [4]. With respect to the traditional Hydroelectric power plants, Darrieus water turbines have the advantage of simplicity. In fact, in contrast to conventional hydroelectric turbines, where an artificial water-head is created using dams (for large-hydro) or penstocks for (micro-hydro), hydrokinetic converters, which convert the kinetic energy of moving river or tide water into electrical energy, are constructed without significantly altering the natural pathway of the water stream [5].

Marco Raciti Castelli is a Research Associate at the Department of Mechanical Engineering of the University of Padua, Via Venezia 1, 35131 Padova, Italy (e-mail: marco.raciticastelli@unipd.it).

Stefano De Betta has completed his M.Sc. in Aerospace Engineering at the University of Padua, Via Venezia 1, 35131 Padova, Italy.

Ernesto Benini is an Associate Professor at the Department of Mechanical Engineering of the University of Padua, Via Venezia 1, 35131 Padova, Italy (e-mail: ernesto.benini@unipd.it).

For the development of water turbines, much can be learned from experience with wind turbines, even if different operating boundary conditions, like fluid density and kinematic viscosity, must be taken into account. Besides, since the operating fluid is water, cavitation can eventually occur. Moreover, the main advantage of the troposkien-shaped blades on a wind turbine, consisting in the great reduction of bending moments, is largely lost in water because, unlike the air, water dynamic forces on blades typically exceed centrifugal forces, so the blades are in compression and will tend to buckle on the upstream pass [6].

As pointed out by Kirke and Lazauskas [6], one of the disadvantages of the Darrieus water turbine is the shaking. In fact, fixed pitch Darrieus turbines tend to vibrate, due to the cyclical variation of the angle of attack, with each blade experiencing two peaks in both radial and tangential force per revolution. The variation in tangential force affects the transmission while the variation in radial force affects the support structure, and if this frequency coincides with the natural frequency of the support structure it can be destructive. One method to reduce the torque oscillations and the intensity of the radial fluid-dynamic forces is to increment the blade number, as presented in this work.

Kyozuka [7] investigated the adoption of a Darrieus water turbine for tidal current power generation, verifying that, thanks to the higher density of water, the current can have a velocity much lower than air to produce the same amount of energy. In fact, since the density of water is 800 times greater than air density and the power of the flow is proportional to the cube of the fluid velocity, the power of an ocean current of 2 knots is equal to a wind flow of 9 m/s.

Khan et al. [8] provided a comparison of hydro and wind turbines, observing that wind turbines are usually designed to operate with rated wind speed of 11-13 m/s. On the contrary, river turbines with augmentation channels, adopted with the aim of enhancing the total volumetric water flow and subsequent power output, could be designed for effective water velocities of 1.75-2.25 m/s or even higher, depending on the site resources. This suggested the possibility of a higher energy generation capacity potential of a river turbine, compared to an equally sized wind energy conversion system.

The main geometrical characteristics of a Darrieus water turbine are the blade shape, the number of blades and consequently the solidity, defined as:

$$\sigma = Nc / R_{rotor} \quad (1)$$

where N is blade number [-], c is blade chord [m] and R_{rotor} is rotor radius [m]. As pointed out by Howell et al. [9], solidity is one of the main parameters dictating the rotational velocity at which the turbine reaches its maximum performance: through

experimental studies, the behavior of both two and three-bladed VAWTs was compared, proving that the two-bladed configuration was able to generate an higher power than the three-bladed architecture.

Li and Li [10] made a series of numerical analysis to investigate the effect of solidity on a straight-bladed vertical axis wind turbine, changing both blade chord and blade number. It was registered that VAWTs characterized by a large solidity were able to achieve the maximum power at lower tip speed ratio. However, a too large solidity determined a decrease of the power coefficient. Furthermore, even for the same solidity, the different combination of blade number and chord affected the power performance of VAWTs greatly. The same behavior can be assumed for a VWaterT: in this work, two-dimensional CFD simulations of the flow field around tree-bladed, four-bladed and five-bladed Darrieus rotors are performed, with the aim of determining the influence of blade number on the performance of the turbine. The solutions are obtained using unstructured moving grids, rotating with the same angular velocity of rotor blades. For each configuration, the flow field characteristics are investigated at several values of the tip speed ratio, in order to analyze the changes in rotor power-curves due to the variation of blade number.

II. Model Geometry

The aim of the present work is to numerically analyze the aerodynamic behavior of a three, four and five-bladed Darrieus VAWaterT operating at different angular velocities, for a constant current of 2 m/s. The main geometrical features of the examined rotors are summarized in Table I.

TABLE I
MAIN GEOMETRICAL FEATURES OF THE ANALYZED ROTORS

Denomination	Value
D_{rotor} [mm]	1030
H_{rotor} [mm]	1 (2D simulation)
Blade profile	NACA 0025
c [mm]	85.8

The solidity parameter σ was defined as suggested by Strickland [11]. For the candidate three, four and five-bladed rotor configurations, its values are respectively 0.5, 0.67 and 0.83.

Rotor azimuthal position was identified by the angular coordinate of the pressure centre of blade No. 1 (set at 0.25·c for NACA 0025 airfoil), starting between the 2nd and 3rd Cartesian plane octants, as can be seen from Fig. 1.

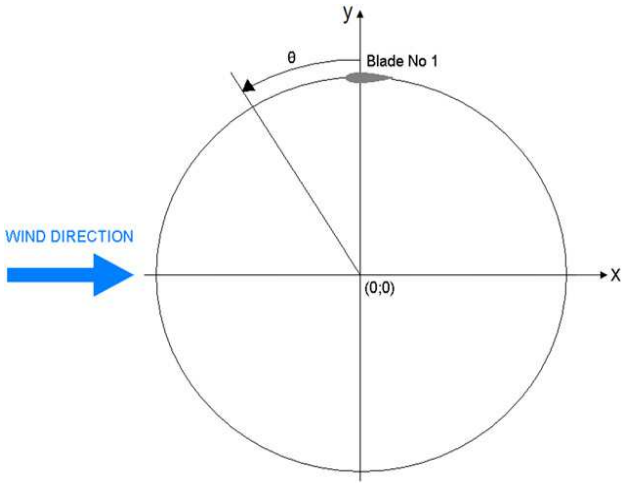

Fig. 1 Azimuthal coordinate of blade No.1 center of pressure

III. Description of the Numerical Flow Field

As the aim of the present work was to reproduce the operation of a rotating machine, the use of moving sub-grids was necessary. In particular, the discretization of the computational domain into macro-areas led to two distinct sub-grids:

- a rectangular outer zone, determining the overall calculation domain, with a circular opening centered on the turbine rotational axis, which was identified as *Domain sub-grid*, fixed;
- a circular inner zone, which was identified as *Rotor sub-grid*, rotating with rotor angular velocity ω.

Fig. 2 shows the main dimensions of the *Domain sub-grid* area.

In order to allow a full development of the wake, Ferreira et al. [12] placed inlet and outlet boundary conditions respectively 10 diameters upwind and 14 diameters downwind with respect to rotor test section for a wind tunnel CFD simulation. In the present study, due to the huge domain width necessary to avoid solid blockage, inlet and outlet were placed respectively 37 rotor diameters upstream and 60 rotor diameters downstream with regard to the rotor test section. Inlet was set as a *velocity inlet*, with a constant velocity profile of 2 m/s, while outlet was set as a *pressure outlet*. Two *symmetry* boundary conditions were used for the two side walls. The circumference around the circular opening, centered on the turbine rotational axis, was set as an *interface*, thus ensuring the continuity of the flow field.

The *Rotor sub-grid* area was characterized by a moving mesh, rotating at the same angular velocity of the turbine. Its location coincided exactly with the circular opening inside the *Domain sub-grid* area and was centered on the turbine rotational axis. Fig. 3 shows the main dimensions and the boundary conditions of the *Rotor sub-grid* area. All blade profiles inside this area were enclosed in a control circle of 400 mm diameter. Unlike the *interface*, it had no physical significance: its aim was to allow a precise dimensional control of the grid elements in the area close to rotor blades, by adopting a first size function operating from the blade profile to the control circle itself and a second size function operating

from the control circle to the whole *Rotor sub-grid* area, ending with grid elements of the same size of the corresponding *Domain sub-grid* elements. An *interior* boundary condition was used for control circle borders, thus ensuring the continuity of the cells on both sides of the mesh.

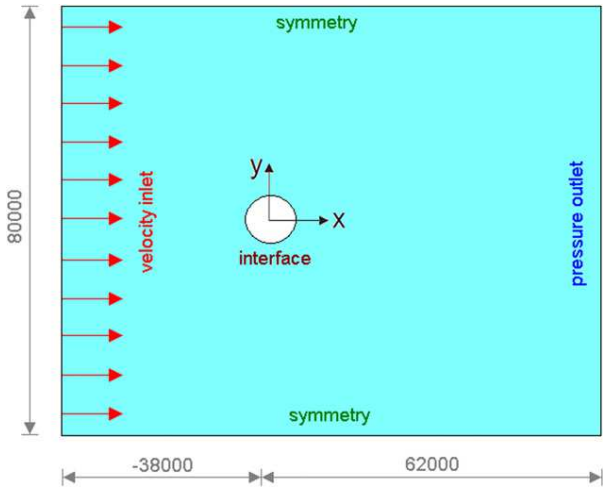

Fig. 2 Main dimensions [mm] of the *Domain sub-grid* area

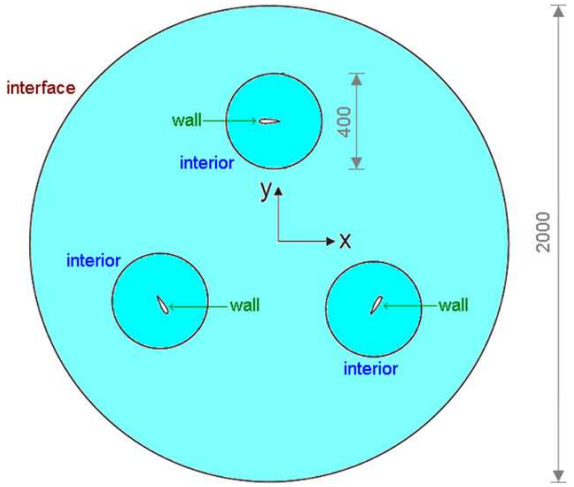

Fig. 3 Schema of the *Rotor sub-grid* area [mm] for three-bladed VAWaterT architecture

IV. Discretization of the Numerical Flow Field

A sliding mesh was adopted in order to reproduce the rotational motion of the VAWaterT. To discretize the flow field, an unstructured grid was chosen for the entire domain, in order to reduce the engineering time to prepare the CFD simulations. The mesh on both sides of the interface (*Rotor sub-grid* and *Domain sub-grid* areas) had approximately the same characteristic cell size, in order to obtain faster convergence [13]. An isotropic unstructured mesh was chosen for the *Rotor sub-grid*, in order to guarantee the same accuracy in the prediction of rotor's performance during the revolution of the turbine (according to the studies of Commings et al. [14]) and also in order to test the prediction capability of a very simple grid. Considering their features of flexibility and adaption capability, unstructured meshes are in fact very easy to obtain, for complex geometries, too, and often represent the "first attempt" in order to get a quick response from the CFD in engineering work. The *Rotor sub-grid* mesh is represented in Fig. 4 for the five-bladed turbine architecture.

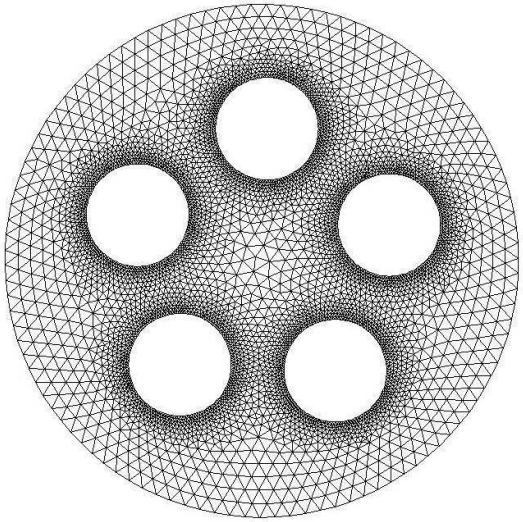

Fig. 4 Rotor sub-grid mesh for the five-bladed VAWaterT architecture

TABLE II
Main Geometrical Dimensions of the Computational Domain

Denomination	Value
Starting grid size from airfoil leading edge [mm]	13
Growth factor from airfoil leading edge [-]	1.08
Starting grid size from airfoil trailing edge [mm]	0.4
Growth factor from airfoil trailing edge [-]	1.28
Maximum grid size on airfoil [mm]	3.5
Growth factor from airfoil surface to *Rotor sub-grid* area [mm]	1.25
Maximum grid size on Rotor sub-grid area [mm]	10

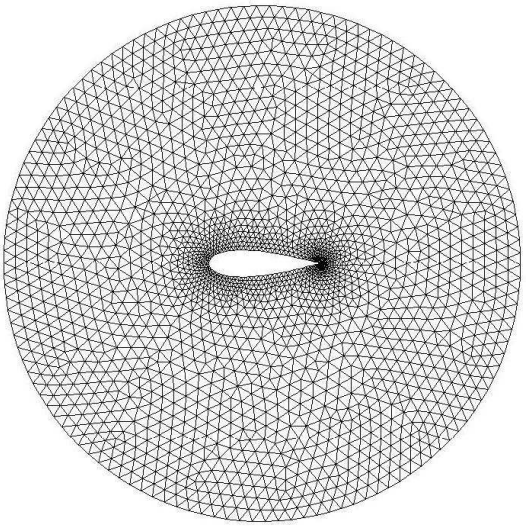

Fig. 5 Control circle grid for NACA 0025 blade section

Being the area close to the blade profiles, great attention was placed in the control circle. The computational grids were constructed from lower topologies to higher ones, adopting appropriate size functions, in order to cluster grid points near the leading edge and the trailing edge of the blade profile, so as to improve the CFD code capability of determining lift, drag and the separation of the flow from the blade itself. Table II summarizes the main features of the mesh close to rotor blade, while Fig. 5 represents the control circle mesh.

V. Numerical Code Settings and Turbulence Model Selection

As observed by McMullen et al. [15], the calculation of unsteady flows in turbomachinery continues to present a severe challenge to CFD. During VAWaterT operation, the unsteadiness stems mainly from the relative motion of the rotating blade and has a fundamental period which depends both on the rate of rotation and on the number of blades. For the proposed calculations, the temporal discretization was achieved by imposing a physical time step equal to the lapse of time the rotor takes to make a 1° rotation.

As a global convergence criterion, each simulation was run until instantaneous torque values showed a deviation of less than 1% compared with the equivalent values of the previous period, for three consecutive periods. The period resulted a function of the number of blades, corresponding to a revolution of 120°, 90° and 72° respectively for three, four and five-bladed rotor architectures. Residuals convergence criterion for each physical time step was set to 10^{-5}, as suggested by Raciti Castelli et al. [16].

As observed by Yu et al. [17], for airfoil flows with great adverse pressure gradient and separation, the choice of a turbulence model is very important. The *k-ω SST* turbulence model can achieve good results because of its capability of capturing proper behaviour in the near wall layers and separated flow regions. In the case of low Reynolds numbers, laminar-to-turbulent transition is also an important factor that should be taken into account, in order to more accurately predict the flow separation and skin friction. In the present work, the chosen turbulence model was the *k-ω SST*, that combines several desirable elements of the existing two-equation models. A 2D pressure based solver was adopted, which is well suited to solve incompressible flows [13]. The unsteady formulation was set to second-order implicit.

VI. Results and Discussion

Fig. 6 represents the evolution of the power coefficient of the three analyzed rotor architectures, defined as:

$$C_p = P / (\tfrac{1}{2}\rho A V_\infty^3) \quad (2)$$

as a function of the tip speed ratio, for an incident water current of 2 m/s. As can be clearly seen, the peak of power coefficient lowers and moves towards lower tip speed ratio with the increase of rotor solidity. This means that a larger number of blades allows the shifting of the maximum power coefficient for lower angular speeds, but is penalized as far as efficiency is concerned.

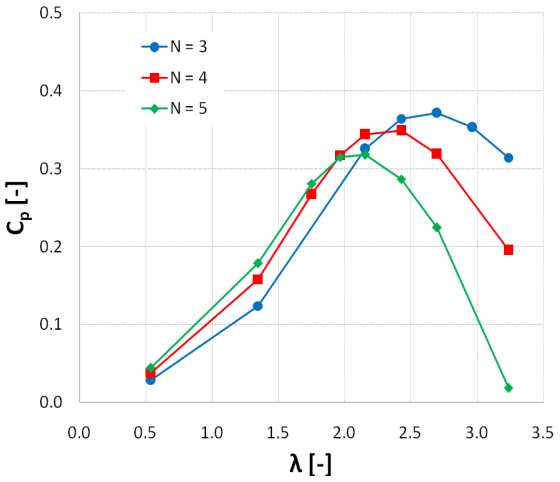

Fig. 6 Rotor power coefficient as a function of the tip speed ratio

The peak power coefficients registered for the three analyzed rotor configurations are presented in Table III. Adopting the power coefficient of the three-bladed turbine as a reference, a 6% performance decrease is registered for the four-bladed configuration, while the five-bladed architecture exhibits a 14% lowering in the performance. The value of the optimal tip speed ratio is lowered of 10% for the four-bladed configuration and of 20% for the five-bladed architecture. The reduction of the optimal tip speed ratio appears to be a much important issue for a water turbine than it could be for a wind turbine, because it is connected with the cavitation phenomenon, which appears at high values of blade tangential velocity.

TABLE III
Peak power coefficients and corresponding tip speed ratios for the three candidate blade architectures

N [-]	$\lambda_{Cp,max}$	$C_{p,max}$
3	2.70	0.36
4	2.43	0.34
5	2.16	0.31

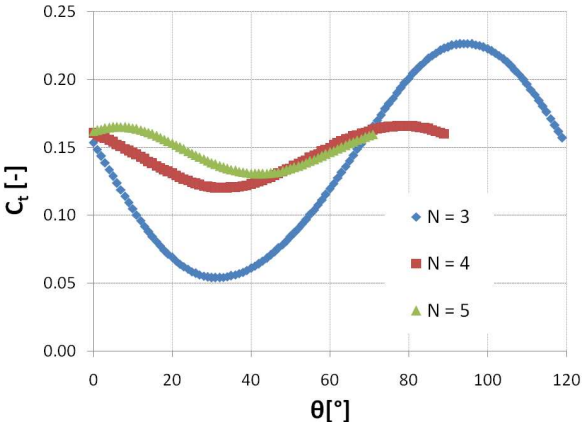

Fig. 7 Rotor torque coefficient as a function of the angular position of blade No. 1 (single period plotted), optimal tip speed ratio (λ=2.70 for N=3, λ=2.43 for N=4, λ=2.16 for N=5)

TABLE IV
AVERAGE, MAXIMUM AND MINIMUM VALUES OF THE TORQUE COEFFICIENT FOR THE THREE ANALYZED ROTOR CONFIGURATIONS

N [-]	$C_{t,avg}$ [-]	$C_{t,max}$ [-]	$C_{t,min}$ [-]
3	0.14	0.23	0.05
4	0.14	0.17	0.12
5	0.15	0.17	0.13

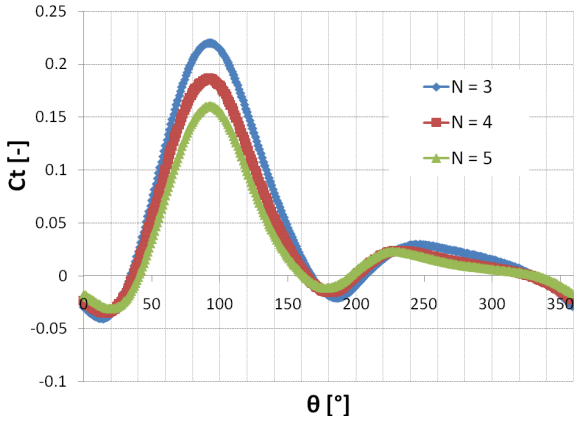

Fig. 8 Instantaneous torque coefficients of blade No. 1 as a function of its azimuthal coordinate, optimal tip speed ratio (λ=2.70 for N=3, λ=2.43 for N=4, λ=2.16 for N=5)

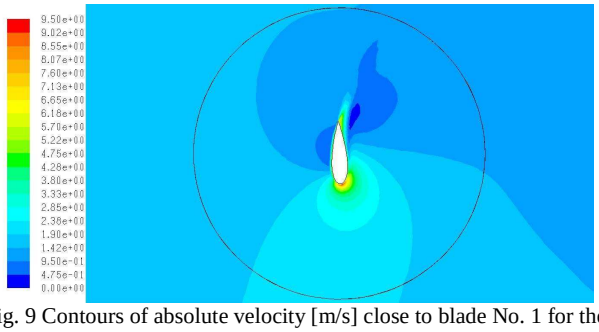

Fig. 9 Contours of absolute velocity [m/s] close to blade No. 1 for the angular position of maximum torque coefficient (θ=92°), N=3, λ=2.70

Fig. 7 shows the torque coefficient, defined as:

$$C_t = T / (½\rho A R_{rotor} V_\infty^2) \quad (3)$$

as a function of the angular position of blade No. 1 (only a single period of revolution is represented for each rotor configuration). As can be clearly noticed, with the increase of rotor blade number, the torque coefficient peaks become lower and the frequency of the oscillations in the torque is increased, due to the higher number of periods during a full rotor revolution. The average, maximum and minimum values of C_t, for the three analyzed rotors and for the tip speed ratios of maximum power coefficient, are represented in Table IV. It can be seen that the increase of blade number determines a reduction in the oscillations of the torque coefficient, while its average value remains almost constant.

Fig. 8 shows the relation between the azimuthal position and the torque coefficient of blade No. 1. It can be seen that the maximum torque values are generated during the upstream revolution of the turbine and for azimuthal positions where rotor blades are experiencing very high relative angles of attack, even beyond the stall limit, as already observed by Raciti Castelli et al. [16] for a wind turbine airfoil. The angular position of maximum instantaneous torque coefficient is 92° for all the three examined cases.

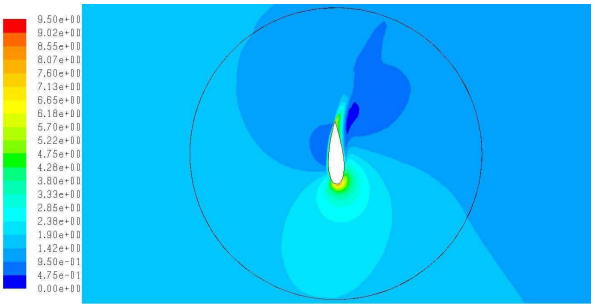

Fig. 10 Contours of absolute velocity [m/s] close to blade No. 1 for the angular position of maximum torque coefficient (θ=92°), N=4, λ=2.43

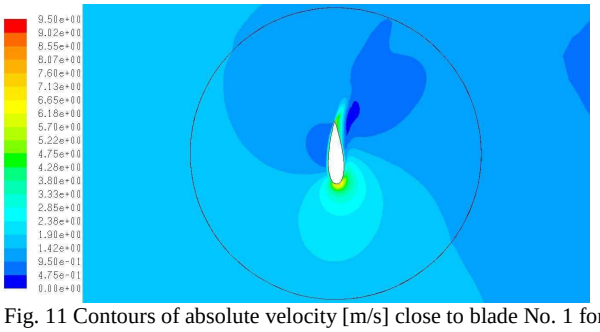

Fig. 11 Contours of absolute velocity [m/s] close to blade No. 1 for the angular position of maximum torque coefficient (θ=92°), N=5, λ=2.16

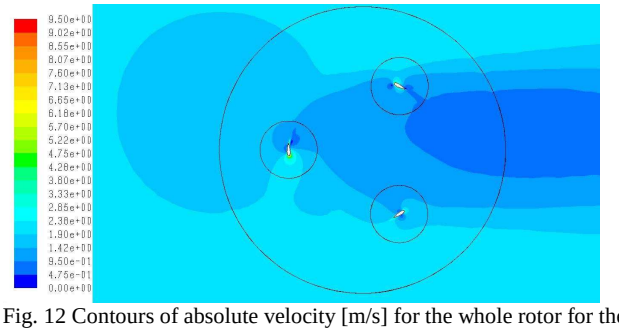

Fig. 12 Contours of absolute velocity [m/s] for the whole rotor for the angular position of maximum torque coefficient (θ= 92°), N=3, λ=2.70

The contours of absolute velocity around the blade No. 1, for the position of maximum torque coefficient and for the three analyzed rotor configurations are shown in Figs. 9, 10 and 11. As can be clearly seen, no significant variations are registered.

Figures 12, 13 and 14 represent the contours of absolute velocity for the whole rotor area. Again, no significant variations are registered; probably due to the fact that the tip

speed ratios of optimum power coefficient resulted relatively close each other.

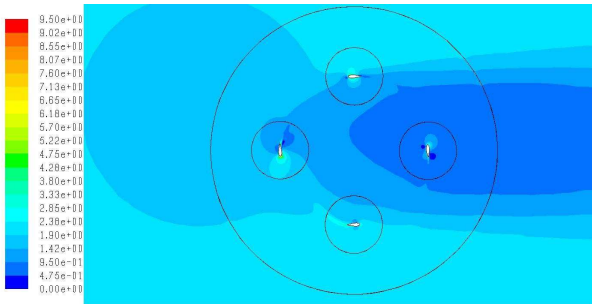

Fig. 13 Contours of absolute velocity [m/s] for the whole rotor for the angular position of maximum torque coefficient (θ= 92°), N=4, λ=2.43

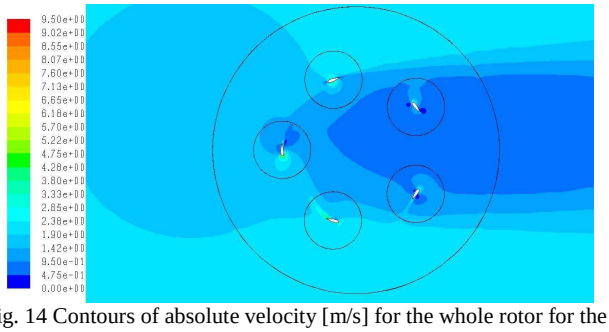

Fig. 14 Contours of absolute velocity [m/s] for the whole rotor for the angular position of maximum torque coefficient (θ= 92°), N=5, λ=2.16

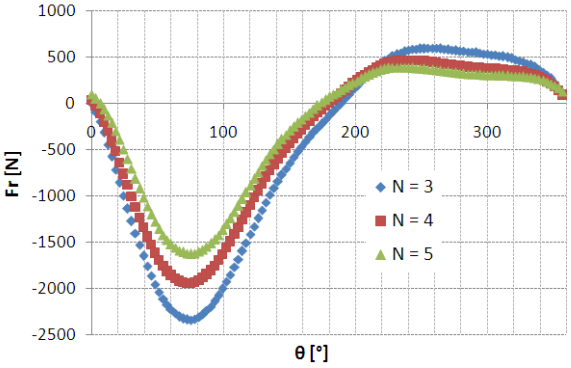

Fig. 15 Hydro-dynamic radial force on a single blade as a function of the azimuthal coordinate (the force is considered as negative if the airfoil is pushed towards the rotor axis), optimal tip speed ratio (λ=2.70 for N=3, λ=2.43 for N=4, λ=2.16 for N=5)

Figure 15 shows the effect of the increment of blade number on the hydro-dynamic radial force acting on blade No. 1 over an entire revolution. This component of the resultant force acting on the airfoil does not produce any effect on the torque of the rotor, but its amplitude can cause structural damages. As can be clearly seen, the increment of blade number achieved a reduction of the peak of the radial force. Table V presents the values of the maximum radial force and the variation with respect to the radial force obtained for the three bladed rotor (as the aim of this work is to investigate the effect of the blade number on the fluid-dynamic of the blade, the centrifugal force has been neglected).

TABLE V
PEAK ABSOLUTE VALUES OF MAXIMUM RADIAL FORCE AND PERCENTAGE DIFFERENCES WITH RESPECT TO THE THREE BLADED ROTOR CONFIGURATION

N [-]	$F_{r,max}$ [N]	$\Delta F_{r,max}$ [%]
3	-2335.3	-
4	-1944.5	-16.7
5	-1627.2	-30.3

VII. Conclusions and Future Work

A full campaign of numerical analyses was performed in order to investigate the effect of blade number on the performance of a straight-bladed VAWaterT. The adoption of a higher number of blades allowed to reach the maximum power coefficient for lower angular velocities, but was penalized as far as efficiency is concerned. The observed percentage differences between peak-power coefficients resulted quite similar to that obtained by Raciti Castelli et al. [18] [19] for a vertical-axis wind turbine: in fact, the fluid-dynamic effect obtained increasing the blade number resulted similar to what occurs with the inclination of a three-dimensional blade.

It was proved that VAWaterTs with a large number of blades can reduce torque fluctuations and minimize vibrations. Nevertheless, turbines with blades inclined to the flow can also reduce or overcome the vibration problem because blade profiles do not stall along their full length simultaneously: further work should be done, in order to analyze the combined effect of the increment in blade number and blade inclination, through a series of complete three-dimensional analysis.

Also the torque coefficient of the rotor presented a lowering, passing from three to five blades, while the frequency of torque oscillations increased.

Small differences were registered, between the three analyzed rotor architectures, in the flow field close to a single hydrofoil for the position of maximum torque coefficient. This phenomenon can be due to the proximity of the tip speed ratios at which the peak of torque occurs.

Finally, it was proved that, increasing the blade number leads to a reduction of the hydro-dynamic radial force on rotor blades, which is much desirable from a structural perspective. Further analysis should be done to investigate the combined effect of hydro-dynamic radial force and centrifugal force on the structural behaviour of rotor blades. Also the percentile differences in normal force passing from three to five blades resulted similar to that obtained by Raciti Castelli et al. [18].

Acknowledgement

The present work was developed in cooperation with Vortex Energy S.r.l. (Italy), as a part of a research project finalized to the manufacturing of a Darrieus VAWaterT.

NOMENCLATURE

A [m^2]	rotor swept area
c [m]	blade chord
C_t [-]	water turbine torque coefficient
C_p [-]	water turbine power coefficient
D_{rotor} [m]	rotor diameter
F_r [N]	hydro-dynamic radial force
$F_{r,max}$ [N]	maximum radial force acting on a single blade during a full rotor revolution
H_{rotor} [m]	rotor height
N [-]	number of blades
P [W]	water turbine power output
Re [-]	Reynolds number
R_{rotor} [m]	rotor radius
T [Nm]	water turbine torque output
V_∞ [m/s]	free-stream current velocity
θ [°]	azimuthal position
$\Delta F_{r,max}$ [%]	maximum radial force percentage deviation with respect to rotor three-bladed configuration
λ [-]	tip speed ratio
μ [Pa·s]	water dynamic viscosity
ρ [kg/m^3]	water density
σ [-]	rotor solidity
ω [rad/s]	rotor angular velocity

REFERENCES

[1] I. Parschivoiu, *Wind Turbine Design: With Emphasis on Darrieus Concept*, Presses Internationales Polytechnique, Montreal, 2002.

[2] G. J. M. Darrieus, "Turbine having its Rotating Shaft Transverse to the Flow of the Current", *U.S. Patent No. 1,835,018*, issued on Dec. 8, 1931.

[3] M. J. Khan, M. T. Iqbal and J. E. Quaicoe, "Design Considerations of a Straight Bladed Darrieus Rotor for River Current Turbines", *IEEE International Symposium on Industrial Electronics*, Montreal (Quebec), 9-13 July, 2006.

[4] Y. M. Dai and W. Lam, "Numerical study of straight-blade Darrieus-type tidal turbine", *Energy* 162, May 2009.

[5] M. J. Khan, G. Bhuyan, M. T. Iqbal and J. E. Quaicoe, "Hydrokinetic energy conversion systems and assessment of horizontal and vertical axis wind turbines for river and tidal applications: A technology status review", *Applied Energy* 86, pp. 1823-1835, 2009.

[6] B. K. Kirke and L. Lazauskas, "Limitations of fixed pitch Darrieus hydrokinetic turbines and the challenge of variable pitch", *Renevable Energy* 36, pp. 893-897, 2011.

[7] Y. Kyozuka, "An Experimental Study on the Darrieus-Savonius Turbine for the Tidal Current Power Generation", *Journal of Fluid Science and Technology*, Vol. 3, pp.439-449, 2008.

[8] M. J. Khan, M. T. Iqbal and J. E. Quaicoe, "River current energy conversion systems: Progress, prospects and challenges", *Renewable and Sustainable Energy Reviews* 12, pp. 2177-2193, 2008.

[9] R. Howell, N. Qin, J. Edwards and N. Durrani, "Wind tunnel and numerical study of a small vertical axis wind turbine", *Renewable Energy* 35, 2010.

[10] S. Li and Y. Li, "Numerical study on the performance effects of solidity on the straight-bladed vertical axes wind turbine", Asia-Pacific Power and Energy Engineering Conference (APPEEC), Chengdu (China), 28-31 March, 2010.

[11] J. H. Strickland: "The Darrieus turbine: a performance prediction model using multiple streamtube", *SAND 75e0431*, 1975.

[12] S. Ferreira, H., Bijl, G. van Bussel and G. van Kuik, "Simulating dynamic stall in a 2D VAWT: modeling strategy, verification and validation with particle image velocimetry data", *Journal of Physics*: Conference Series 75 (2007), 012023.

[13] Fluent Inc., *Fluent User's Manual*, pp. 193-194, 2006.

[14] R. M. Cummings, J. R. Forsythe, S. A. Morton and K. D. Squires, "Computational challenges in high angle of attack flow prediction", *Progress in Aerospace Sciences*, Vol. 39, No. 5. (July 2003), pp. 369-384.

[15] M. McMullen, A. Jameson and J. J. Alonso, "Acceleration of convergence to a periodic steady state in turbomachinery flows", *39th AIAA Aerospace Sciences Meeting & Exhibit*, Reno (Nevada), January 8-11, 2001.

[16] M. Raciti Castelli, A. Englaro and E. Benini, "The Darrieus wind turbine: Proposal for new performance prediction model based on CFD", *Energy*, Volume 36, Issue 8, August 2011.

[17] G. H. Yu, X. C. Zhu and Z. H. Du, "Numerical simulation of a wind turbine airfoil: dynamic stall and comparison with experiments", *Power and Energy Journal*, Vol. 224, 2010.

[18] M. Raciti Castelli, S. De Betta and E. Benini, "Effect of Blade Number on a Straight-Bladed Vertical-Axis Darrieus Wind Turbine", *World Academy of Science, Engineering and Technology*, Issue 61, January 2012, pp. 305-311.

[19] M. Raciti Castelli, E. Benini, Effect of Blade Inclination Angle on a Darrieus Wind Turbine, *Journal of Turbomachinery*, May 2012, Vol. 134, 031016-1-10.